Block Copolymers of Styrene and Stearyl Methacrylate. Synthesis and Micellization Properties in Selective Solvents

Marinos Pitsikalis, Ekaterini Siakali-Kioulafa, and Nikos Hadjichristidis*

Department of Chemistry, University of Athens, Panepistimiopolis Zografou, 15771 Athens, Greece

Received February 11, 2000; Revised Manuscript Received May 8, 2000

ABSTRACT: Block copolymers of styrene and stearyl methacrylate were prepared using anionic polymerization high-vacuum techniques by sequential addition of monomers. Narrow molecular weight distribution copolymers of different molecular weight and composition were obtained. The molecular characteristics of the copolymers were obtained by size exclusion chromatography, membrane osmometry, low-angle laser light scattering (LALLS), and differential scanning calorimetry. Comparative studies in the selective solvents for the polystyrene block, ethyl and methyl acetate, showed that mainly unimolecular micelles are formed in the former, whereas larger aggregates are observed in the latter solvent. LALLS, viscometry, and dynamic light scattering were used to characterize the micelles.

Introduction

It is well-known that when block copolymers are dissolved in a selective solvent, supramolecular assemblies, called micelles are formed.[1−3] The behavior of micellar solutions has been the subject of numerous studies,[4] due to their applications in coatings, drug delivery systems, colloid stabilization, nanoreactors,[5−8] etc.

In most cases the micelles are spherical, consisting of the core which contains the segregated insoluble blocks and the shell of the soluble blocks which surrounds the core.[9] The micellization process is considered as an equilibrium between unassociated single chains, the unimers, and the micelles.[10−14] A more complicated situation exists when some insoluble blocks are not fully integrated into a single micellar core, but are partly incorporated into two cores, thus acting as bridges between two micelles. This phenomenon, called micellar clustering, has frequently been observed, especially in more complex systems such as triblock and graft copolymers.[15] The equilibrium of unimers, micelles, and clusters is very difficult to analyze, and the combination of several experimental techniques is required to study these complex systems.[16−24] Most important are the scattering techniques (static and dynamic light scattering, neutron scattering, small-angle X-ray scattering), but also other methods such as membrane osmometry (MO), viscometry, electron microscopy, nuclear magnetic resonance spectroscopy (NMR), sedimentation velocity and fluoresence techniques, and size exclusion chromatography (SEC) have also been used.

In this paper we report on the synthesis and characterization of polystyrene-*b*-poly(stearyl methacrylate), PS-*b*-PSMA, block copolymers and their micellization behavior in solvents that are selective for the PS blocks, i.e., ethyl (EAc) and methyl acetate (MAc). The synthesis of these copolymers was first reported by Teyssié et al.[25] In Teyssié's work diblocks having molecular weights up to 26 000, high PSMA contents (>50%), and rather broad molecular weight distributions ($M_w/M_n \geq 1.75$) were presented. These copolymers were used to stabilize dispersions of carbon black in an organic solvent, selective for the PSMA block.

Many studies have appeared in the literature concerning the micelle properties of copolymers consisting of a PS and a polymethacrylate block.[26−28] Most of these referred to polystyrene-*b*-poly(methyl methacrylate),[29−32] PS-*b*-PMMA, copolymers, either in single selective solvents (e.g., *p*-xylene, acetone) or in solvent mixtures (e.g., toluene/*p*-cumene, toluene/furfuryl alcohol). In general, high degrees of aggregation were observed; the micelles obtained were mainly spherical, and in a few cases more extended ellipsoidal or cylindrical shaped micelles were present.

An important characteristic of the system under the present investigation is the ability of the PSMA side chains to form crystalline domains.[33] The micellization properties of amorphous−crystalline block copolymers have not been examined theoretically in detail. A similar system that has been studied is the micellization of polystyrene-*b*-poly(ethylene oxide), PS-*b*-PEO, diblocks in organic solvents.[34−37] It was found that when dry solvents selective for the PS blocks are used, unusually large structures are formed, probably due to the crystallizability of the PEO chains that form the core of the micelles.[38]

Experimental Section

Materials. The polymer synthesis and almost all the purification techniques were performed in vacuum, in all-glass reactors provided with break-seals and constrictions.[39] The purification of tetrahydrofuran (THF), styrene (S), and 1,1-diphenylethylene (DPE) to the standards required for anionic polymerization has been described elsewhere.[39] Stearyl methacrylate (SMA) was recrystallized three times from hexane at −30 °C. The solid monomer was placed in an ampule and was thoroughly dried in the vacuum line for at least 24 h. The monomer was then dissolved in THF to yield a 5% solution, by distilling the appropriate amount of the solvent through the vacuum line. *sec*-Buli was prepared under vacuum in glass reactors by reacting *sec*-BuCl with Li metal in hexane. Lithium chloride (LiCl) was placed in ampules, flame-dried under vacuum, and dissolved in THF just prior to polymerization. Degassed methanol was used to terminate the living polymers. EAc and MAc were dried over CaH_2 and distilled just prior to use.

Polymer Synthesis. The polymerization was carried out in the appropriate glass reactors, bearing ampules of S, SMA in THF, DPE, *sec*-BuLi in hexane, LiCl, and methanol. The desired amount of THF was distilled into the polymerization

10.1021/ma0002646 CCC: $19.00 © 2000 American Chemical Society
Published on Web 07/06/2000

apparatus, which was then sealed off from the vacuum line. The flask was cooled to −78 °C in a dry ice−2-propanol bath. *sec*-BuLi was introduced into the reactor, breaking the suitable break-seal, and the polymerization of styrene was initiated by breaking the styrene ampule and distilling the monomer into the reactor. The polymerization took place under vigorous stirring using a glass stirrer. After the polymerization was completed, the DPE solution (3-fold excess over the concentration of the living ends) was added. The color rapidly changed from orange to deep red. A few minutes later the LiCl solution (5-fold excess over the concentration of the living ends) was added (no color change was observed), and the break-seal of the ampule containing the SMA solution was ruptured. The monomer solution was added dropwise into the living polymer solution at −78 °C. The monomer droplets were immediately frozen, and thus the temperature was raised to −10 °C. Upon increasing the temperature the deep red color suddenly disappeared, due to the initiation of the polymerization of SMA. The solution was transparent at −10 °C throughout the whole polymerization procedure. Finally the living polymer was deactivated by adding degassed methanol. The polymer was precipitated in excess methanol. All polymers were fractionated using toluene/methanol as the solvent/nonsolvent system in order to avoid any homopolymer contamination.

Preparation of the Micellar Solutions. The dry polymers were dissolved in EAc or MAc for the preparation of the stock solution. After standing for 24 h the solution was placed in an oven at 50 °C for 1 h in order to achieve equilibrium structures and then was left for 24 h at room temperature before conducting the appropriate measurements. The stock solution was diluted to produce solutions of different concentrations. No polymer precipitation or other visible changes were observed after standing at room temperature for several weeks.

Characterization Methods. SEC experiments were conducted at 40 °C using a modular instrument consisting of a Waters model 510 pump, a Waters model U6K sample injector, a Waters model 401 differential refractometer, a Waters model 486 UV spectrophotometer, and a set of 4 μ-Styragel columns with a continuous porosity range from 10^6 to 10^3 Å. THF was the carrier solvent at a flow rate of 1 mL/min.

A Jupiter model 231 membrane osmometer was used for the determination of the number-average molecular weights, M_n, and second virial coefficients, A_2, at 35 °C. Toluene distilled over CaH_2 was used as the solvent.

Static light scattering measurements were performed with a Chromatix KMX-6 low-angle laser light scattering photometer at 25 °C equipped with a 2 mW He−Ne laser operating at $\lambda = 633$ nm.

Refractive index increments, dn/dc, at 25 °C were measured with a Chromatix KMX-16 refractometer operating at 633 nm. The dn/dc dependence on the polymer composition in THF, EAc, and MAc is given by the following equations: $(dn/dc)_{THF} = 0.080 + 0.108w_{PS}$, $(dn/dc)_{EAc} = 0.130 + 0.092w_{PS}$, and $(dn/dc)_{MAc} = 0.167 + 0.043w_{PS}$, where w_{PS} is the polystyrene weight fraction.

Dynamic light scattering measurements were conducted with a series 4700 Malvern system composed of a PCS5101 goniometer with a PCS stepper motor controller, a Cyonics variable power Ar^+ laser, operating at 488 nm, a PCS8 temperature control unit, a RR98 pump/filtering unit, and a 192-channel correlator for the accumulation of the data. The correlation functions were analyzed by the cumulant method and the CONTIN software. Measurements were carried out at 45°, 90°, and 135°. The angular dependence of the ratio Γ/q^2, where Γ is the decay rate of the correlation function and q is the scattering vector, was not very important for the micellar solutions, due to their large sizes.

The viscosity measurements were carried out at 25 °C using Cannon-Ubbelohde dilution viscometers with a Scott-Geräte AVS 410 automatic flow timer and were analyzed using the Huggins and the Kraemer equation.

Polymer melting points were obtained by differential scanning calorimetry (DSC) using a 2910 modulated DSC model from TA Instruments. The samples were heated or cooled at a rate of 10 °C/min.

Results and Discussion

A. Synthesis and Characterization. Diblock copolymers of styrene (S) and stearyl methacrylate (SMA) are symbolized as SSMA followed by two numbers corresponding to the total weight-average molecular weight and the weight percent composition in styrene, as found by UV-SEC. The synthesis of the samples was conducted by anionic polymerization and sequential addition of the two monomers, according to the reaction scheme in Chart 1. There are two characteristic difficulties associated with the anionic polymerization of SMA, i.e., the purification of the monomer and its insolubility in THF at −78 °C. The classical way for the purification of methacrylates is by treating the monomer over CaH_2 and triethylaluminum (TEA) or trioctylaluminum (TOA), which react with the protonated impurities (water, alcohols, or acids) and by distillation of the purified monomer to glass ampules.[40] This procedure is very difficult to employ for stearyl methacrylate since the monomer has a very high boiling point (>310 °C at 1 atm), and consequently, a considerable amount of polymerization is observed when trying to distill the purified monomer from TEA or TOA to the glass ampules.[41]

To overcome this problem, the first attempt was to titrate the impurities by the dropwise addition of TOA into a solution of SMA in THF. The appearance of a pale greenish yellow color, due to the formation of the TOA−SMA complex, was considered to be the end point of the titration. This monomer solution was directly used for the preparation of sample SSMA 47/55. No detectable trace of the PS block, which could possibly been deactivated upon the addition of the SMA, was observed; i.e., the methacrylate monomer was pure enough, according to the standards of anionic polymerization. Nevertheless, a small amount of gelation and a tailing effect were observed at the higher molecular weight region of the chromatogram, indicating that a small amount of cross-linked and/or a higher molecular weight sample was also formed, due to the presence of a small excess of TOA in the system. It seems that the color of the TOA−SMA complex is not a very sensitive indication of the end point of the titration of the impurities and that a considerable amount of TOA still remains in the solution, which is able to lead to formation of cross-linked and/or higher molecular weight products. Fractionation of the initial sample SSMA 47/55 yielded the final product with the molecular weight polydispersity reduced from 1.18 to 1.10.

Because of these difficulties, a much simpler technique of purification was used, the recrystallization of the monomer from hexane at −30 °C. The monomer was recrystallized three times, placed in an ampule, and then left on the vacuum line to be dried overnight. Finally the monomer was diluted with THF. Characteristic chromatograms of the samples prepared by this method are given in Figure 1. Narrow molecular weight distribution copolymers were observed for all samples. To further check whether this purification method is adequate for the standards of anionic polymerization, a high molecular weight sample SSMA 500/86 was prepared. The very low concentration of the living centers, needed for the synthesis of this high molecular weight polymer, makes them very sensitive to the

Chart 1

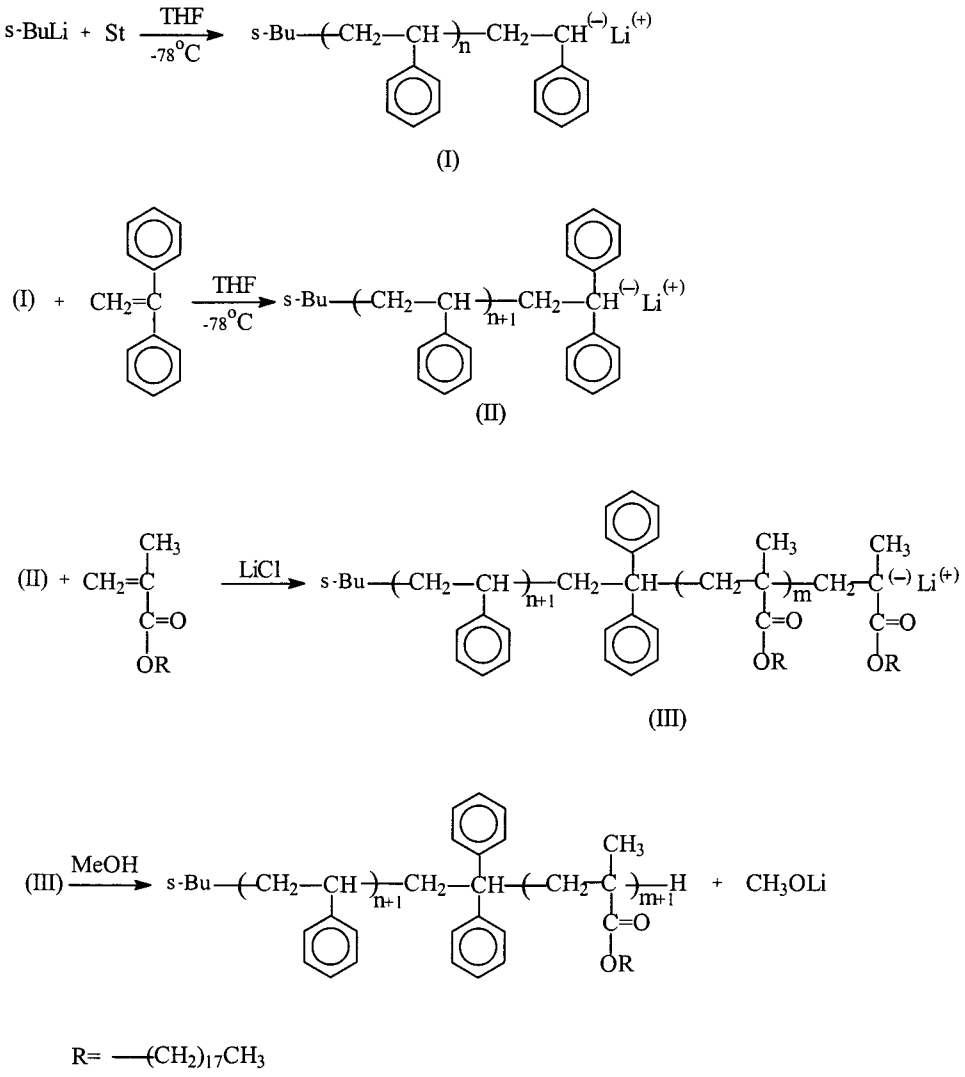

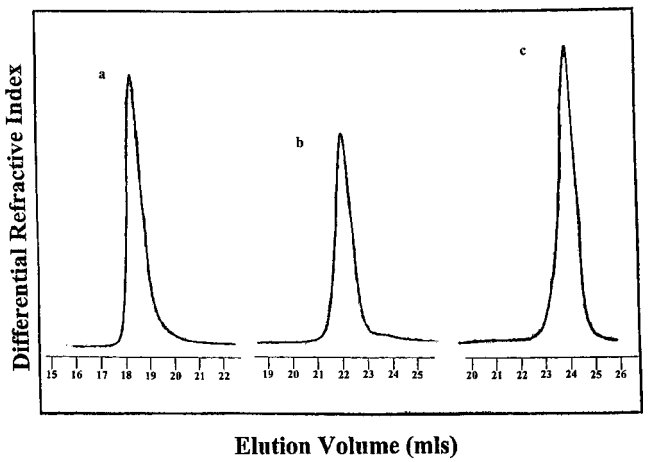

Figure 1. SEC chromatograms of samples: (a) SSMA 500/86, (b) SSMA 90/83, (c) SSMA 30/74.

impurities that can be introduced by the addition of the SMA solution. As can be seen in Figure 1a, only a small tailing at the lower molecular weight region was observed, suggesting that less than 5% of PS was terminated upon the addition of the SMA. This result associated with the low molecular weight distribution of the samples indicates that recrystallization is an efficient purification method.

The second major difficulty in the polymerization of the SMA is its insolubility in THF at −78 °C. The same problem was also faced by Teyssié et al.[25] It was concluded that the best solution was to perform the polymerization at −10 °C, where the reaction was homogeneous. It is known from previous studies that low polymerization temperatures (usually −78 °C) are required for the living polymerization of methacrylates, to suppress the side reactions at the reactive carbonyl group.[42] Only in the case of *tert*-butyl methacrylate (*t*-BuMA) higher polymerization temperatures, i.e., −30 °C, were used.[43] The bulky side group seems to protect the carbonyl group. A similar situation probably exists in the case of the polymerization of SMA. The long alkyl group act as a protective shield against the side reactions. When the polymerizations were conducted by careful control of the reaction temperature at −10 °C, the molecular weights measured by MO and LALLS were very close to the stoichiometric. Nevertheless, at temperatures higher than −10 °C the polymerization is susceptible to side reactions. For example, homopolymerization of SMA was conducted at 0 °C in the presence of LiCl. Although the stoichiometric molecular weight was $M_s = 25\,000$, the observed molecular weight by SEC was $M_w = 17\,000$ and the molecular weight distribution was $M_w/M_n = 1.4$, showing that termination reactions took place during the polymerization.

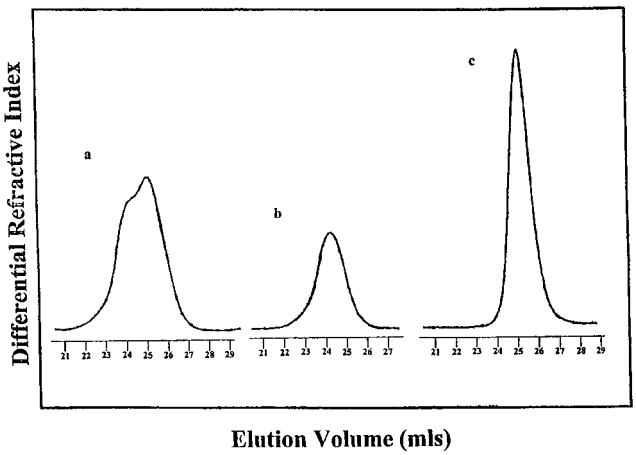

Figure 2. SEC chromatograms from the synthesis of the PS-*b*-PSMA-*b*-PS triblock copolymer: (a) crude product, (b) pure triblock after fractionation, (c) excess diblock copolymer.

Table 1. Molecular Characteristics of the Triblock PS-*b*-PSMA-*b*-PS Copolymer

sample	M_n[a]	A_2[a] × 10^4 (mL mol g^{-2})	I[b] (M_w/M_n)	wt % PS[c]
PS-*b*-PSMA-PS	29 400	7.2	1.12	43.5
PS-*b*-PSMA	15 300	9.1	1.14	43.6

[a] By MO in toluene at 35 °C. [b] By SEC. [c] By UV-SEC.

The presence of LiCl in the polymerization mixture seems to be responsible for the narrow molecular weight polydispersities of the copolymers. Teyssié et al. reported distributions as high as 1.80 for their samples, in the absence of LiCl. Similar behavior was also observed in other cases[44−48] and was interpreted by assuming that in the absence of LiCl associated and nonassociated ion pairs are present in the solution. Their reactivity is very different, and since both species interconvert very slowly, they lead to different polymerization rates upon the addition of the monomer and thus broad molecular weight distributions. In the presence of LiCl the equilibrium between the associated and the nonassociated ion pairs is much faster. Thus, LiCl helps the system to be depleted from the slowly interconverting aggregates, leading to the formation of monodisperse polymers.

The living character of the polymerization was further checked by linking the living diblocks with dibromomethylbenzene. It was recently reported[49] that bromomethylbenzene derivatives can be successfully used as linking agents for the preparation of PMMA and P*t*BuMA stars with four branches and PS-*b*-poly(*tert*-butyl acrylate)-*b*-PS, PS-*b*-PtBuA-*b*-PS triblock copolymers. In the present study a triblock copolymer PS-*b*-PSMA-*b*-PS was synthesized by linking the living PS-*b*-PSMALi solution with dibromomethylbenzene. The chromatograms obtained after the synthesis of the triblock polymer are given in Figure 2. A large excess of the living diblock was used, and the linking reaction was allowed to take place for 5 days at −10 °C. The SEC chromatogram of the crude product showed two peaks. This product was fractionated to give the triblock copolymer and the excess diblock. The molecular characteristics of the two samples, given in Table 1, show that the triblock copolymer was efficiently prepared by this method.

A detailed molecular characterization for all samples is listed in Table 2. The molecular weight distributions obtained by SEC were very close to the ratio M_w/M_n obtained by MO (M_n) and LALLS (M_w) measurements. The distribution increases by increasing the SMA content and reaches the value 1.18 for the sample SSMA 62/11 which has 89.2% of SMA. As a precaution, and in order to avoid contamination of the samples with homopolymers, fractionation was performed. Middle fractions were collected in all cases. The molecular weight distributions for all fractions of the same sample were almost identical. In addition, similar narrow molecular weight distributions were observed in SEC using both refractive index and UV detectors, indicating that the samples are chemically and compositionally homogeneous. The compositions were calculated by UV-SEC and range from 10 to 90 wt % in PS.

B. Thermal Properties. Several studies concerning the crystallization behavior of polymethacrylates with long alkyl side groups have been published.[50−52] In a recent paper the conformational and crystallization behavior of the PSMA was reported using SAXS and dielectric spectroscopy.[53]

The case of diblock copolymers consisting of a crystallizable and an amorphous block was examined theoretically by Flory.[54] Using a lattice model, he analyzed the thermodynamics of crystallization of homopolymers and copolymers. For the latter case he predicted a decrease of the melting point of the crystallizable block compared to that of the pure homopolymer. This melting point depression, according to Flory, is influenced by the length of the crystallizable block and the thermodynamic interactions between the two blocks.

The experimental results from the PS-*b*-PSMA blocks are reported in Table 3. The characteristic melting endotherms corresponding to the melting of the crystallites is evident in almost all samples. The glass transition temperature, T_g, of the PS block corresponds to the expected value having in mind the dependence of the T_g with respect to the molecular weight of the linear PS.[55] The T_g of the PSMA was reported in the literature[56,57] to be very low (−100 °C) and observed as a weak transition, due to the crystallinity of the polymer. For these reasons the T_g of the PSMA blocks could not be easily detected with accuracy, but it was very low in all cases. From the results shown in Table 3 it is obvious that the samples are microphase separated, due to the observation of both the PSMA melting points and the PS T_g values, which are very close to the expected ones considering the molecular weight dependence of the T_g of PS. This result is further supported by the data obtained by Ruzette et al.[58] concerning the phase behavior of block copolymers consisting of polystyrene and poly(*n*-alkyl methacrylates) having up to 12 carbon atoms. The interaction parameter, χ, increased with the length of the alkyl side group of the polymethacrylate block. Specifically in the case of the PS-*b*-poly(lauryl methacrylate) diblocks an average χ value of 0.083 was calculated by SANS in the temperature range 150−210 °C. Samples with molecular weight as low as 30 000 were microphase separated at temperatures lower than 200 °C. This effect is expected to be more pronounced in the case of the PS-*b*-PSMA diblocks.

As was predicted by Flory and observed experimentally in other studies,[59−61] the T_m values for the copolymers are lower than that of the homopolymer. In one sample (SSMA 500/86) no crystallinity was found, due to the very low PSMA content (13.8 wt %). This result

Table 2. Molecular Characteristics of the PS-*b*-PSMA Diblock Copolymers

sample	M_n[a]	A_2[a] × 10^4 (mL mol g^{-2})	M_w[b]	A_2[b] × 10^4 (mL mol g^{-2})	wt % PS[c]	I[d] (M_w/M_n)
SSMA 47/55	43 500	5.79	47 300	5.00	55.2	1.10
SSMA 500/86			464 500	3.24	86.2	1.08
SSMA 90/83	88 100	4.66	88 800	5.07	83.1	1.04
SSMA 32/76	30 200	6.97	32 000	8.95	75.6	1.05
SSMA 62/11	51 700	4.88	62 400	3.21	10.8	1.18
SSMA 42/68	38 500	6.14	42 600	7.05	67.8	1.05
SSMA 30/74	28 600	10	30 200	9.15	74.2	1.06

[a] By membrane osmometry (MO) in toluene at 35 °C. [b] By low-angle laser light scattering (LALLS) in THF at 25 °C. [c] By UV-SEC. [d] By size exclusion chromatography (SEC).

Table 3. DSC Results of the PS-*b*-PSMA Diblock Copolymers

sample	T_g,[a] °C PS	T_m,[a] °C PSMA	ΔH_m,[a] J/g SMA
SSMA 47/55	83.5	30.6	37.9
SSMA 500/86	101.0		
SSMA 90/83	70.0	29.7	9.5
SSMA 32/76	86.0	24.7	13.8
SSMA 62/11	92.3	27.7	54.7
SSMA 42/68	89.0	21.8	14.2
SMA[b]		34.0	75.9

[a] Second heating results. [b] Linear PSMA with $M_w = 17\,000$ by SEC.

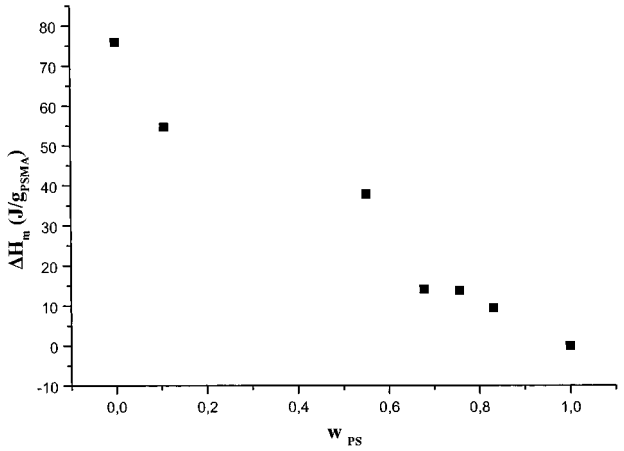

Figure 3. Normalized enthalpy of melting, ΔH_m, vs the composition in PS.

is in agreement with previous studies[62,63] and with the observation that the normalized enthalpy of melting decreases by increasing the PS content. These results are plotted in Figure 3.

It is obvious that even for the sample with 10.8 wt % PS an almost 28% enthalpy loss was calculated. This effect can be attributed either to the existence of fuzzy boundaries between the PS and PSMA regions and/or to an irregular structure at the interface so that the PSMA segments near the phase boundary are in a disordered state, and only the segments in the interior of its microphase take part in the crystallization. Further study is required to clarify this phenomenon.

C. Micellization in Selective Solvents. The micellization properties of the PS-*b*-PSMA block copolymers were studied in EAc and MAc. It is known that propyl acetate is a θ-solvent at 36 °C;[64] EAc and MAc are nonsolvents for PSMA. The solubility parameters of EAc and MAc, δ, are 9.1 and 9.6 $(cal/cm^3)^{1/2}$, respectively, whereas the corresponding values for the PS and the PSMA homopolymers are 9.3 and 7.8 $(cal/cm^3)^{1/2}$, respectively.[55] From the above it is concluded that both solvents are selective solvents for PS. Consequently, micelles are expected to be formed in these solvents consisting of PSMA cores and PS coronas. The micellar properties were studied by static and dynamic light scattering and by viscometry.

Low-Angle Laser Light Scattering. The LALLS data of the PS-*b*-PSMA diblocks in EAc are given in Table 4. These results show that the weight-average degree of association, N_w, defined as the ratio of the M_w measured in the selective solvent over the M_w of the diblock in the common good solvent THF is equal to unity in most cases. Only when the PSMA content is higher than 45 wt % (sample SSMA 47/55) polymolecular micelles are formed. It is characteristic that the sample SSMA 62/11 with almost 90 wt % PSMA is insoluble in EAc. Since EAc is a nonsolvent for PSMA, promoting the micellization of the block copolymers with high contents of PSMA and A_2 has low values even for the samples with $N_w \sim 1$; unimolecular micelles are formed in the case of samples with low PSMA contents, and only by increasing the polymethacrylate content multimolecular micelles are formed. The formation of unimolecular micelles has been previously observed in the literature in the case of multiblock copolymers and graft copolymers in selective solvents for the branches.[65−67] Unimers of diblock copolymers have been observed especially when they are in equilibrium with polymolecular micelles. More evidence about the formation of unimolecular micelles will be provided in subsequent sections.

The LALLS plot for sample SSMA 47/55 is linear over the concentration range examined; i.e., the critical micelle concentration, cmc, is much lower than the lowest experimentally accessible concentration (~5 × 10^{-4} g/mL), and stable micellar structures exist in that concentration regime.

Table 4. Low-Angle Laser Light Scattering Data of the PS-*b*-PSMA Diblock Copolymers in Ethyl and Methyl Acetate

	ethyl acetate			methyl acetate		
sample	M_w	A_2 × 10^4 (mL mol g^{-2})	N_w[a]	M_w	A_2 × 10^6 (mL mol g^{-2})	N_w[a]
SSMA 47/55	1 415 000	0.028	29.5			
SSMA 500/86	467 000	1.1	1.0	625 000	−8.3	1.34
SSMA 32/76	32 200	7.4	1.0_1	966 500	3.7	30.2
SSMA 42/68	43 200	1.7	1.0_1	549 000	−6.4	12.9
SSMA 30/74	30 500	1.2	1.0_1	800 000	2.4	26.5

[a] Weight-average degree of association.

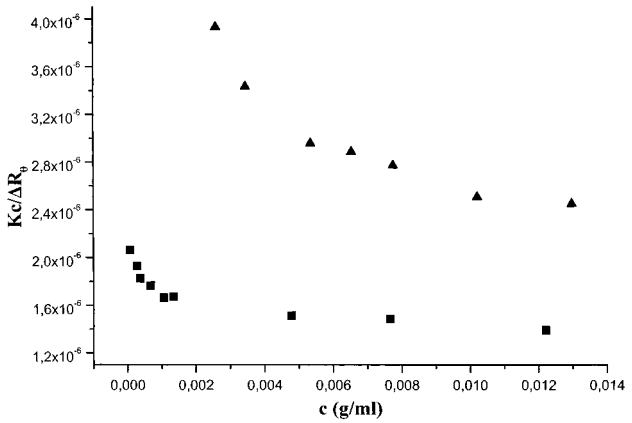

Figure 4. LALLS plots for samples SSMA 500/86 (■) and 42/68 (▲) in MAc.

A different situation was observed when MAc was used as selective solvent. Multimolecular micellar solutions with the characteristic blue color were obtained in almost all cases. The LALLS data are presented in Table 4, whereas characteristic plots are given in Figure 4. It is characteristic that diblocks with higher PSMA contents (SSMA 47/55 and SSMA 62/11) were insoluble in this solvent even after thermal treatment at 50 °C. Only the sample with the lowest PSMA content, SSMA 500/86, shows a small tendency for the formation of multimolecular micelles. It seems that the large PS block solubilizes the PSMA core so that the system forms mostly unimolecular rather than multimolecular micelles. The characteristic LALLS plot (Figure 4) and the negative A_2 value are indicative of the presence of strong intramolecular interactions and consequently unimolecular micelles. The degrees of association for the other diblocks are of the same order of magnitude and seem to be sensitive to both the PSMA content and the total molecular weight of the sample. As in the case of EAc, no cmc value could be detected, despite the fact that the characteristic concentration region where the micelles are organized could be observed in all cases.

Viscometry. Dilute solution viscometry measurements were performed in the common good solvent THF at 25 °C. The results are reported in Table 5. The rather high k_H values obtained are due to the comblike structure of the PSMA block and are consistent with the data reported for the PSMA homopolymers.[64]

The data collected in EAc are presented in Table 5 and confirm the conclusions drawn by LALLS. The formation of multimolecular micelles from sample SSMA 47/55 is evident by the large increase in the viscometric radius and the much higher k_H value, which indicates the existence of strong hydrodynamic interactions. The Huggins and Kraemer plots are given in Figure 5.

The existence of unimolecular micelles in EAc for the samples with the lower PSMA content is manifested from the higher k_H values and the lower $[\eta]$ and R_v values compared to the corresponding results in THF.

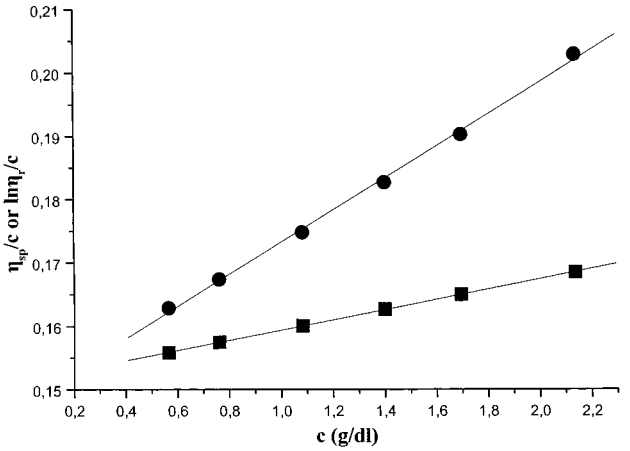

Figure 5. Huggins (●) and Kraemer (■) plots for sample SSMA 47/55 in EAc.

Especially the R_v values are 10−12.5% lower than those in THF. This difference is systematic for all the samples and cannot be attributed to experimental errors or the difference in quality of the two solvents (EAc and THF) for the PS blocks, since both have the same solubility parameter.

The viscometry results in MAc are presented in Table 5. In all cases the k_H values are very high, indicating the existence of strong hydrodynamic interactions, even in the case of sample SSMA 500/86, where the degree of association is almost unity. The viscometric radius is 28% lower for this sample compared to the value obtained in THF, indicating that mostly unimers exist in MAc, in agreement with the LALLS data.

The results from the other samples show that the intrinsic viscosities are lower and the viscometric radii higher than in THF meaning that more compact structures occur in this solvent.

Dynamic Light Scattering. The dynamic light scattering (DLS) results in THF for the PS-*b*-PSMA copolymers are presented in Table 6. Positive k_D values were observed in all cases.

As is expected, the R_h values are similar to the corresponding R_v values obtained by viscometry in THF.

The corresponding DLS data for the diblock copolymers in EAc are given in Table 6. The samples with the lower PSMA content have R_h values which are lower, up to 12%, compared to those measured in THF, and their k_D values are negative in all cases. This result is in agreement with the low A_2 values obtained in EAc, since k_D and A_2 are related through the equation:

$$k_D = 2A_2M + k_f - u \qquad (1)$$

where M is the molecular weight, k_f the coefficient of the concentration dependence of the friction coefficient, and u the partial specific volume of the polymer. Because of the similar molecular weights in both solvents, THF and EAc, a decrease in A_2 is accompanied

Table 5. Viscometry Results of the PS-*b*-PSMA Diblock Copolymers in THF, Ethyl Acetate, and Methyl Acetate

	THF			ethyl acetate			methyl acetate		
sample	$[\eta]$, dL g^{-1}	k_H	R_v, nm	$[\eta]$, dL g^{-1}	k_H	R_v, nm	$[\eta]$, dL g^{-1}	k_H	R_v, nm
SSMA 47/55	0.248	0.49	5.70	0.148	1.16	14.9			
SSMA 500/86	1.35	0.39	21.5				0.370	1.34	15.4
SSMA 32/76	0.177	0.57	4.46	0.127	0.84	3.96	0.105	1.16	11.7
SSMA 42/68	0.171	0.50	4.78	0.121	0.71	4.18	0.100	1.27	8.82
SSMA 30/74	0.155	0.55	4.20	0.114	0.74	3.78	0.094	1.35	10.6

Table 6. DLS Data for the PS-*b*-PSMA Diblock Copolymers in THF, Ethyl Acetate, and Methyl Acetate

	THF			ethyl acetate			methyl acetate		
sample	$D_0 \times 10^7$ (cm^2/s)	k_d (mL/g)	R_h (nm)	$D_0 \times 10^7$ (cm^2/s)	k_d (mL/g)	R_h (nm)	$D_0 \times 10^7$ (cm^2/s)	k_d (mL/g)	R_h (nm)
SSMA 47/55[a]	3.79	10.97	6.41	0.16	−21.13	31.5 15.3, 37.8			
SSMA 500/86	1.22	93.24	19.4	-	-	-	4.10	−53.67	14.6
SSMA 32/76[b]	5.15	22.52	4.66	1.28	−13.60	4.01	1.14	79.38	52.39 19.7, 72.8
SSMA 42/68[c]	4.80	6.41	5.05	1.07	−9.66	4.77	7.53[d] (5.45)	−106.9[d] (−32.11)	7.96[d] (11.0) 4.48, 21.0
SSMA 30/74	5.27	14.69	4.56	1.26	−24.79	4.08	3.83	−9.29	15.6

[a] CONTIN analysis in ethyl acetate showed the existence of bimodal distribution. The first peak (15.3 nm) corresponds to the micellar structure and the second (37.8 nm) to the formation of clusters. [b] CONTIN analysis in methyl acetate showed the existence of bimodal distribution. The first peak (19.7 nm) corresponds to the micellar structure and the second (72.8 nm) to the formation of clusters. [c] CONTIN analysis in methyl acetate showed the existence of bimodal distribution. The first peak (4.48 nm) corresponds to unassociated polymer chains and the second (21.0 nm) to the micellar structure. [d] The plot in methyl acetate is not linear. The first results correspond to the lower concentration regime, whereas the results given in parentheses to the higher concentration regime.

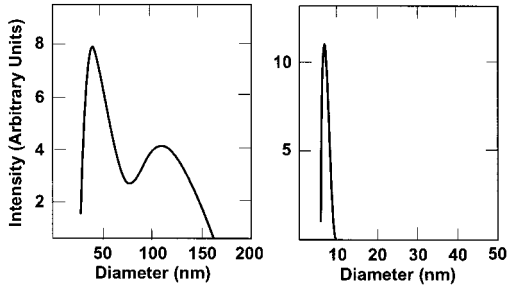

Figure 6. Intensity weighted size distribution by DLS and CONTIN analysis in EAc: (left) sample SSMA 47/55, $\mu_2/\Gamma^2 = 0.23$; (right) sample SSMA 30/74, $\mu_2/\Gamma^2 = 0.05$.

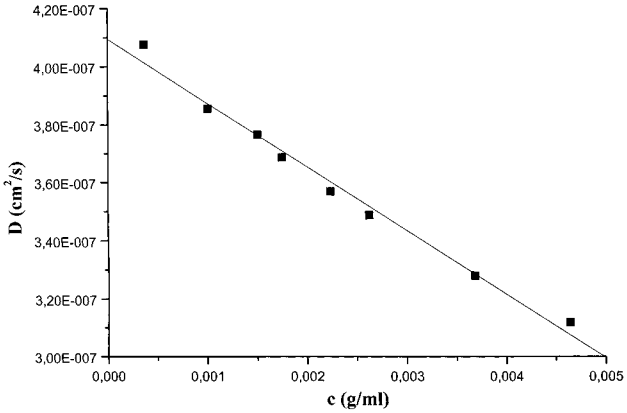

Figure 7. Diffusion coefficient vs concentration plot for sample SSMA 500/86 in MAc.

by a decrease in k_D as well. In addition, the R_h values are in very good agreement with the R_v values obtained by viscometry in EAc. These results provide a further indication that unimolecular micelles are formed in this solvent. Furthermore, these structures are monodisperse as evidenced by the second moment values μ_2/Γ^2 of the cumulant analysis, which were considerably lower than 0.1 for all samples.

A different situation was observed for the sample SSMA 47/55, where multimolecular micelles were observed. Using the CONTIN analysis, a bimodal distribution was obtained. An example from the intensity weighted distributions for samples SSMA 47/55 and SSMA 30/74 is provided in Figure 6. In the concentration range used, the analysis showed the existence of two peaks corresponding to R_h values equal to 15.3 and 37.8 nm. Both values are higher than the one observed in THF (6.41 nm). A possible explanation is that the first peak corresponds to micellar structures, whereas the second one to clusters. Formation of clusters has been observed many times in micellar solutions. In cases where the cores are not very compact and are close to each other, i.e., at increased concentrations, there is a possibility that they start to interpenetrate, giving rise to micellar clusters. The thermal treatment of the samples at 50 °C probably causes a swelling of the cores, thus giving them the opportunity to interact leading to the formation of clusters that remain in the solution after the temperature is lowered to 25 °C.

A similar behavior was obtained in the case of PS-*b*-PEO diblock copolymers in cyclopentane, a solvent selective for the PS blocks.[38] Upon heating the sample to 68 °C, above the melting temperature of the PEO only single chains were observed. Subsequent cooling to 23 °C resulted in the formation of very large aggregates after 24−48 h, which were in equilibrium with micellar structures.

The CONTIN analysis revealed that the solution contains ~60% of clusters. Since the intensity weighted distributions are very much influenced by the large scatterers, it is obvious that the content of clusters is highly overestimated by this method. The micelles were found to be monodisperse, whereas the clusters were polydisperse as judged by the high values of the second moment results of the cumulant analysis ($\mu_2/\Gamma^2 > 0.2$). This is another evidence that the two peaks correspond to micelles and clusters, respectively.

The micellar hydrodynamic radius is in good agreement with the viscometric radius, indicating that the shear forces applied in the capillary tube of the viscometer are able to break the clusters. Similar behavior has been reported in other micellar[68] and aggregating[69] systems and provides evidence that the forces leading to the formation of the clusters are very weak compared to those that are responsible for the formation of the micelles.

The DLS data concerning the hydrodynamic behavior of the PS-*b*-PSMA diblocks in MAc are given in Table 6. As was concluded by LALLS and viscometry, the sample SSMA 500/86 tends to form unimolecular micelles. Figure 7 shows that the k_D value is strongly negative and also the structures are monodisperse ($\mu_2/\Gamma^2 < 0.1$ for all concentrations and angles), as shown in Figure 8, and the hydrodynamic radius is almost 25% lower than that measured in THF. A similar reduction in size was observed by viscometry going from the common good solvent, THF, to the selective solvent,

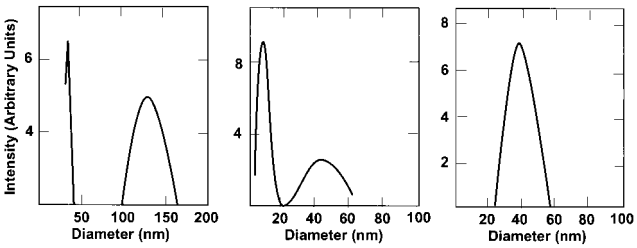

Figure 8. Intensity-weighted size distribution by DLS and CONTIN analysis in MAc: (left) sample SSMA 32/76, $\mu_2/\Gamma^2 = 0.30$; (middle) sample SSMA 42/68, $\mu_2/\Gamma^2 = 0.50$; (right) sample SSMA 500/86, $\mu_2/\Gamma^2 = 0.06$.

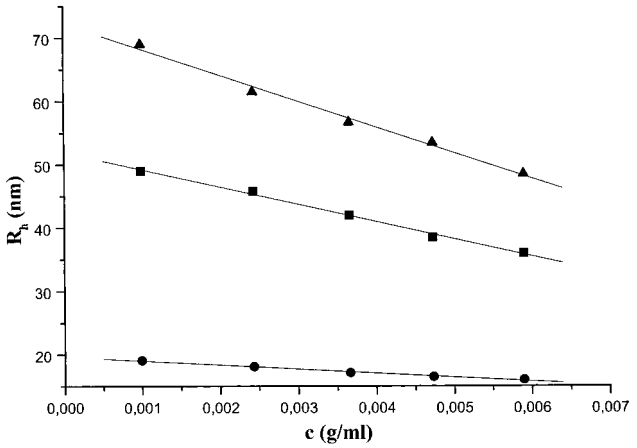

Figure 9. Hydrodynamic radius of micelles (●), clusters (▲), and average values (■) vs concentration for sample SSMA 32/76 in MAc.

MAc. The R_h value is in very good agreement with the R_v value in MAc.

More complicated results were obtained for the samples with the lower PSMA content. The sample SSMA 32/76 displays a bimodal distribution, as shown by the CONTIN analysis, in Figure 8. Both peaks and the average signal give R_h values that scale linearly with concentration and positive k_D values, as shown in Figure 9, indicating that the decrease in the A_2 values is overbalanced by the increased molecular weights in MAc (eq 1). The first peak is near monodisperse corresponding to the micellar structures. The second peak is polydisperse with a much higher R_h value and can be attributed to the formation of clusters. As was pointed out in the case of sample SSMA 47/55 in EAc, these clusters are connected through weak forces and thus can be disrupted by the shear forces developed during the flow in the capillary tube of the viscometer.

The sample SSMA 30/74 also displays a bimodal distribution at lower angles, but at higher angles (>90°) the two peaks merge to one at concentrations higher than 1.5×10^{-3} g/mL as shown in Figure 10. The first peak is near monodisperse and can be attributed to the formation of micelles. The second peak is polydisperse, has a much higher R_h value, and corresponds to micellar clusters. As the two peaks merge, at higher angles the polydispersity factor, μ_2/Γ^2, is reduced from 0.22 to 0.1 by further increasing the concentration. This behavior suggests that the difference in size between micelles and clusters is not as big as in the case of the sample SSMA 32/76 and that by increasing concentration more stable structures are observed. The total k_D value is negative, but higher than the value obtained for the same polymer in EAc, due to the higher molecular weight in MAc.

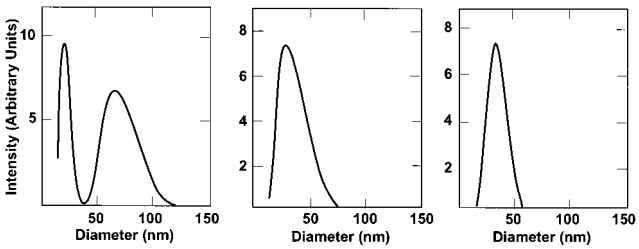

Figure 10. Intensity-weighted size distribution by DLS and CONTIN analysis for sample SSMA 30/74 in MAc: (left) $c = 0.641 \times 10^{-3}$ g/mL, $\mu_2/\Gamma^2 = 0.32$; (middle) $c = 1.539 \times 10^{-3}$ g/mL, $\mu_2/\Gamma^2 = 0.22$; (right) $c = 7.439 \times 10^{-3}$ g/mL, $\mu_2/\Gamma^2 = 0.10$.

DLS data for the sample SSMA 42/68 show that the values of the apparent diffusion coefficient are reduced by increasing concentration. This means that gradually species of lower mobility are formed, which correspond to the development of the micellar structures. The R_h value derived from the high concentration regime is close to the corresponding viscometric radius. CONTIN analysis showed that a bimodal distribution also exists in this case. The first peak has a R_h value very close to the one found for the diblock in THF and is monodisperse. Consequently, it can be attributed to unassociated unimers. The second peak has a much higher R_h value and is polydisperse, thus corresponding to the micellar structures (Figure 8). The R_h values for both the unimer and the micelles scale linearly with concentration, but the content in micelles increases with increasing concentration. The reason for the unimer−micelle equilibrium for this specific copolymer against the more common micelle−cluster equilibrium developed for the other diblocks may be the higher molecular weight of this copolymer and/or the existence of a small amount of PS homopolymer in the sample. The contamination of the final product with a small quantity of PS homopolymer due to partial deactivation of the living PSLi solution upon the addition of the second monomer cannot be ruled out, but it is very difficult to be detected with conventional techniques, because of the low PSMA content.

Micellar Structure. Comparison of these results with other PS-*b*-polymethacrylate copolymers or copolymers consisting of PS and crystalline blocks is not straightforward, due to the differences in solvent quality and the nature of the two blocks. In general, lower aggregation numbers are observed in the system under investigation compared to the PS-*b*-PMMA[29−32] or PS-*b*-poly(methacrylic acid)[70] systems in different selective solvents. Similarly, micellization studies performed using PS-*b*-PEO diblocks in cyclopentane,[38] a selective solvent for the PS block, showed the existence of large aggregates, due to the crystallizability of the PEO blocks and the vicinity to the Θ point of the system PS−cyclopentane. In our case the lower degrees of association can be explained considering on the one hand the different quality of the solvents and on the other hand the long alkyl side chains of PSMA, which probably sterically prevent the main chains to approach each other, thus favoring the formation of micelles with low degrees of aggregation.

Several models have been proposed to describe the micelle structure. The case of micelles consisting of small cores and large coronas can be well described by the star model. If N_A and N_B are the lengths of the corona and core forming blocks A and B, respectively, the star model will be valuable when $N_A \gg N_B$. Accord-

Table 7. Structural Parameters of Micelles

					dry core		swollen core	
sample	R_h, nm	$R_h/(N_B^{4/25}N_A^{3/5})$	$R_h/N_B^{3/5}$	$MA_2/[\eta]$	R_c, nm	A_c, nm^2	R_c, nm	A_c, nm^2
SSMA 47/55[a]	15.3	0.29	0.97	0.27	6.35	17.2	8.00	27.2
SSMA 32/76[b]	19.7	0.45	2.4	0.34	4.57	8.7	5.76	13.8
SSMA 42/68[b]	21.0	0.40	1.8	−0.35	4.15	16.8	5.23	26.6
SSMA 30/74[b]	15.6	0.38	1.9	0.20	4.37	9.0	5.51	14.4

[a] In ethyl acetate. [b] In methyl acetate.

ing to Halperin's star model,[71] the following scaling relationships between the parameters of interest for diblock copolymers can be obtained:

$$\text{aggregation number:} \quad N \sim N_B^{4/5}$$

$$\text{core radius:} \quad R_c \sim N_B^{3/5}$$

$$\text{micelle radius:} \quad R \sim N_B^{4/25} N_A^{3/5}$$

The other limiting case, the situation of micelles consisting of a large core and a relatively thin corona, i.e., when $N_B \gg N_A$, can be described by mean density models.[72−75] According to these models, the volume fraction of the A segments in the corona is assumed to be independent of the distance from the core. The following scaling relationships are obtained:

$$\text{aggregation number:} \quad N \sim N_B$$

$$\text{core radius:} \quad R_c \sim N_B^{2/3}$$

$$\text{micelle radius:} \quad R \sim N_B^{2/3}$$

The low PSMA content of the diblocks examined in this work favor initially the star model. To test these models for the micellar solutions in ethyl and methyl acetate, the ratios $R_h/(N_B^{4/25}N_A^{3/5})$ and $R_h/N_B^{2/3}$ were calculated. The calculations, performed for the samples that form polymolecular micelles, using the R_h values found for the micellar structures are given in Table 7.

From these results it is obvious that the star model is more appropriate to describe the micellar structures. Nevertheless, the ratio $R_h/(N_B^{4/25}N_A^{3/5})$ is not very constant. These deviations may indicate that the micellar core is not very compact. To further test this assumption, the radius of the core was calculated using the equation:

$$R_c = (3M_{w,mic}wt_{PSMA}/4\pi N_A d_{PSMA}\varphi_{PSMA})^{1/3} \qquad (2)$$

where $M_{w,mic}$ is the micellar molecular weight, wt_{PSMA} the weight fraction of the core forming block, d_{PSMA} the density of PSMA, and φ_{PSMA} the volume fraction of PSMA in the core. The density of PSMA was calculated using group contribution methods, according to Van Krevelen[76] ($d_{PSMA} = 0.982 \pm 0.05$). Two limiting cases were considered: the dry core ($\varphi_{PSMA} = 1$) and the swollen core ($\varphi_{PSMA} = 0.5$). The results for both cases are given in Table 7. It is obvious that even in the case of the dry core, the core size is relatively large considering the low PSMA content. The micellar core radii are between 20% and 30% compared to the total R_h values for triblocks containing 26−32% PSMA. This is a direct evidence that that the cores are rather swollen and not very compact.

A rather surprising result is the dependence of R_c on the PSMA block length, N_B. Although the N_B range is rather narrow, it was found in the case of methyl acetate that $R_c \sim N_B^{-4/25}$; i.e., by increasing the length of the PSMA block, the core radius decreases in contrast to the predictions of the model. This behavior can be attributed to the limited range of the N_B values and to the increased tendency for crystallization by increasing the length of the PSMA chains, leading to small contraction of the micelle cores.

It was concluded that for impermeable spheres the following expression is valid:

$$MA_2/[\eta] = 1.6 \qquad (3)$$

The values of $MA_2/[\eta]$ for the micellar solutions are included in Table 7. In almost all cases the values are lower than unity, meaning that these micellar structures cannot be described as impermeable spheres. This result is in agreement with our previous observations that the micelles are not very compact having rather swollen cores.

The area of the core−corona interface, A_c, occupied per copolymer chain is given as

$$A_c = 4\pi R_c^2/N_w \qquad (4)$$

The A_c values for the dry and swollen core cases are reported in Table 7. All of them fall in a relatively narrow range and are similar to those calculated for the micelles formed by the PS-*b*-PMAA copolymers in dioxane/water mixtures 80/20 v/v.

Conclusions

Narrow molecular weight distribution block copolymers of styrene and stearyl methacrylate were prepared by anionic polymerization high-vacuum techniques. Their micellization properties were studied in ethyl and methyl acetate, which are selective solvents for the PS blocks. Unimolecular micelles (intramolecular side group association) are formed in EAc for samples having low PSMA contents. Only when the PSMA content is higher than 45% are multimolecular micelles formed (intermolecular side group association). A similar situation was also observed in MAc. Rather low degrees of aggregation were found in all cases. There is a general trend for the formation of clusters. These structures are not very stable and are disrupted under the influence of the shear forces developed in the capillary viscometer. The micelles are near monodisperse and spherical and have a rather swollen core.

References and Notes

(1) Webber, S. E., Munk, P., Tuzar, Z., Eds. *Solvents and Self-organization of Polymers;* NATO ASI Series Vol. 327.
(2) Tuzar, Z.; Kratochvil, P. *Surf. Colloid Sci.* **1993**, *15*, 1.
(3) Riess, G.; Hurtrez, G.; Bahadur, P. In *Encyclopedia of Polymer Sciences and Engineering*, 2nd ed.; Mark, H., Bikales, N. M., Overberger, C. G., Menges, G., Eds.; John Wiley & Sons: New York, 1985; Vol. 2, pp 324−436.

(4) Munk, P.; Prochazka, K.; Tuzar, Z.; Webber, S. E. *Chem. Technol.* **1998**, 20.
(5) Scholz, C.; Iijima, M.; Nagasaki, Y.; Kataoka, K. *Macromolecules* **1995**, *28*, 7295.
(6) Antonietti, M.; Goltner, C. *Angew. Chem., Int. Ed. Engl.* **1997**, *36*, 910.
(7) Antonietti, M.; Forster, S.; Hartmann, J.; Oesteich, S. *Macromolecules* **1996**, *29*, 3800.
(8) Moffitt, M.; Eisenberg, A. *Chem. Mater.* **1995**, *7*, 1178, 1185.
(9) Price, C.; Hudd, A. L.; Booth, C.; Wright, B. *Polymer* **1982**, *23*, 650.
(10) Watanabe, A.; Matsuda, M. *Macromolecules* **1986**, *19*, 2253.
(11) Major, M. D.; Torkelson, J. M.; Brearley, A. M. *Macromolecules* **1990**, *23*, 1700.
(12) Astafieva, I.; Zhong, X. F.; Eisenberg, A. *Macromolecules* **1993**, *26*, 7339.
(13) Prochazka, K.; Bednar, B.; Mukhtar, E.; Svoboda, P.; Trnena, J.; Almgren, M. *J. Phys. Chem.* **1991**, *95*, 4563.
(14) Wang, Y.; Kausch, C. M.; Chun, M.; Quirk, R. P.; Mattice, W. L. *Macromolecules* **1995**, *28*, 904.
(15) Tuzar, Z.; Konak, C.; Stepanek, P.; Plestil, J.; Kratochvil, P. *Polymer* **1990**, *31*, 2118.
(16) Liu, G. *J. Phys. Chem.* **1995**, *99*, 5465.
(17) Calderara, F.; Hruska, Z.; Hurtrez, G.; Lerch, J.-P.; Nugay, T.; Riess, G. *Macromolecules* **1994**, *27*, 1210.
(18) Cao, T.; Munk, P.; Ramireddy, C.; Tuzar, Z.; Webber, S. E. *Macromolecules* **1991**, *24*, 6300.
(19) Prochazka, K.; Kiserow, D.; Ramireddy, C.; Tuzar, Z.; Munk, P.; Webber, S. E. *Macromolecules* **1992**, *25*, 454.
(20) Kiserow, D.; Prochazka, K.; Ramireddy, C.; Tuzar, Z.; Munk, P.; Webber, S. E. *Macromolecules* **1992**, *25*, 461.
(21) Liu, Y.; Chen, S.-H.; Huang, J. S. *Macromolecules* **1998**, *31*, 2236.
(22) Moffitt, M.; Yu, Y.; Nquyen, D.; Graziano, V.; Schneider, D. K.; Eisenberg, A. *Macromolecules* **1998**, *31*, 2190.
(23) Jorgensen, E. B.; Hvidt, S.; Brown, W.; Schillen, K. *Macromolecules* **1997**, *30*, 2355.
(24) Esselink, F. J.; Dormidontova, E. E.; Hadziioannou, G. *Macromolecules* **1998**, *31*, 4873.
(25) Leemans, L.; Fayt, R.; Teyssié, Ph.; Uytterhoeven, H. *Polymer* **1990**, *31*, 106.
(26) Liu, G.; Smith, C. K.; Hu, N.; Tao, J. *Macromolecules* **1996**, *29*, 220.
(27) Siqueira, D. F.; Nunes, S. P.; Wolf, B. A. *Macromolecules* **1994**, *27*, 4561.
(28) Siqueira, D. F.; Nunes, S. P.; Wolf, B. A. *Macromolecules* **1994**, *27*, 234.
(29) Edwards, C. J. C.; Richards, R. W.; Stepto, R. F. T. *Polymer* **1986**, *27*, 643.
(30) Kotaka, T.; Tanaka, T.; Hattori, M.; Inagaki, H. *Macromolecules* **1978**, *11*, 138.
(31) Utiyama, H.; Takenaka, K.; Mizumori, M.; Fukuda, M.; Tsunashima, Y.; Kurata, M. *Macromolecules* **1974**, *7*, 515.
(32) Duval, M.; Picot, C. *Polymer* **1987**, *28*, 793.
(33) Plate, N. A.; Shibaev, V. P. *J. Polym. Sci., Macromol. Rev.* **1974**, *8*, 117.
(34) Wang, Y.; Kausch, C. M.; Chun, M.; Quirk, R. P.; Mattice, W. L. *Macromolecules* **1995**, *28*, 904.
(35) Candau, S.; Boutillier, J.; Candau, F. *Polymer* **1979**, *20*, 1237.
(36) Xu, R.; Winnik, M. A.; Hallett, F. R.; Riess, G.; Croucher, M. D. *Macromolecules* **1991**, *24*, 87.
(37) Vagberg, L. J. M.; Cogan, K. A.; Gast, A. P. *Macromolecules* **1991**, *24*, 1670.
(38) Cogan, K. A.; Gast, A. P. *Macromolecules* **1990**, *23*, 745.
(39) Morton, M.; Fetters, L. J. *Rubber Chem. Technol.* **1975**, *48*, 359.
(40) Allen, R. D.; Long, T. E.; McGrath, J. E. *Polym. Bull.* **1986**, *15*, 127.
(41) Greenberg, S. A.; Alfrey, T. *J. Am. Chem. Soc.* **1954**, *76*, 6280.
(42) Hsieh, H. L.; Quirk, R. P.; *Anionic Polymerization, Principles and Practical Applications*; Marcel Dekker: New York, 1996.
(43) Muller, A. H. E. *Makromol. Chem.* **1981**, *182*, 2863.
(44) Varshney, S. K.; Gao, Z.; Zhong, X. F.; Eisenberg, A. *Macromolecules* **1994**, *27*, 1076.
(45) Teyssie, P.; Fayt, R.; Hautekeer, J. P.; Jacobs, C.; Jerome, R.; Leemans, L.; Varshney, S. K. *Makromol. Chem., Macromol. Symp.* **1990**, *32*, 61.
(46) Varshney, S. K.; Hautekeer, J. P.; Fayt, R.; Jerome, R.; Teyssié, P. *Macromolecules* **1990**, *23*, 2618.
(47) Kunkel, D.; Muller, A. H. E.; Janata, M.; Lochmann, L. *Macromol. Chem., Macromol. Symp.* **1992**, *60*, 315.
(48) Baumgarten, J. L.; Muller, A. H. E.; Hogen-Esch, T. E. *Macromolecules* **1991**, *24*, 353.
(49) Pitsikalis, M.; Sioula, S.; Pispas, S.; Hadjichristidis, N.; Cook, D. C.; Li, J.; Mays, J. W. *J. Polym. Sci., Polym. Chem. Ed.* **1999**, *37*, 4337.
(50) Jordan, E. F., Jr.; Feldeisen, D. W.; Wrigley, A. N. *J. Polym. Sci., Part A-1* **1971**, *9*, 1835.
(51) Jordan, E. F., Jr.; Bohdan, A.; Speca, A.; Wrigley, A. N. *J. Polym. Sci., Part A-1* **1971**, *9*, 3349.
(52) Jordan, E. F., Jr. *J. Polym. Sci., Part A-1* **1971**, *9*, 3367.
(53) Alig, I.; Jarek, M.; Hellmann, G. P. *Macromolecules* **1998**, *31*, 2245.
(54) Flory, P. J. *J. Chem. Phys.* **1949**, *17*, 223.
(55) Brandrup, J., Immergut, E. H., Eds. *Polymer Handbook*, 2nd ed.; John Wiley & Sons: New York, 1975.
(56) Rogers, S. S.; Mandelkern, L. *J. Phys. Chem.* **1957**, *61*, 985.
(57) Gedde, U. W. *Polymer Physics*, 3rd ed.; Kluwer Academic Publishers: Dordrecht, 1999.
(58) Ruzette, A.-V. G.; Banerjee, P.; Mayes, A. M.; Pollard, M.; Russell, T. P.; Jerome, R.; Slawecki, T.; Hjelm, R.; Thiyagarajan, P. *Macromolecules* **1998**, *31*, 8509.
(59) Mao, G.; Wang, J.; Clingman, S. R.; Ober, C. K.; Chen, J. T.; Thomas, E. L. *Macromolecules* **1997**, *30*, 2556.
(60) Yamada, M.; Iguchi, T.; Hirao, T.; Nakahama, S.; Watanabe, J. *Polym. J.* **1998**, *30*, 23.
(61) Fiecher, H.; Poser, S.; Arnold, M.; Frank, W. *Macromolecules* **1994**, *27*, 7133.
(62) Boussias, C. M.; Peters, R. H.; Still, R. H. *J. Appl. Polym. Sci.* **1980**, *25*, 855.
(63) Castles, L. J.; Vallance, M. A.; McKenna, J. M.; Cooper, S. L. *J. Polym. Sci., Polym. Phys. Ed.* **1985**, *23*, 2119.
(64) Xu, Z.; Hadjichristidis, N.; Fetters, L. J. *Macromolecules* **1984**, *17*, 2303.
(65) Selb, J.; Gallot, Y. *Makromol. Chem.* **1981**, *182*, 1775.
(66) Price, C.; Woods, D. *Polymer* **1973**, *14*, 82.
(67) Spevasec, J. *Makromol. Chem., Rapid Commun.* **1982**, *4*, 697.
(68) Antonietti, M.; Heinz, S.; Schmidt, M.; Rosenauer, C. *Macromolecules* **1994**, *27*, 3276.
(69) Pitsikalis, M.; Hadjichristidis, N. *Macromolecules* **1996**, *29*, 179.
(70) Qin, A.; Tian, M.; Ramireddy, C.; Webber, S. E.; Munk, P.; Tuzar, Z. *Macromolecules* **1994**, *27*, 120.
(71) Halperin, A. *Macromolecules* **1987**, *20*, 2943.
(72) Noolandi, J.; Hong, M. H. *Macromolecules* **1983**, *16*, 1443.
(73) Leibler, L.; Orland, H.; Wheeler, J. C. *J. Chem. Phys.* **1983**, *79*, 3550.
(74) Nagarajan, R.; Ganesh, K. *J. Chem. Phys.* **1989**, *90*, 5843.
(75) Munch, M. R.; Gast, A. P. *Macromolecules* **1988**, *21*, 1360.
(76) Van Krevelen, D. W.; Hoftyzer, P. J. *Properties of Polymers. Correlations with Chemical Structure*; Elsevier: New York, 1972.
(77) Elias, H. G. *Macromolecules*, 2nd ed.; Plenum Press: New York, 1984; Vol. 1.

MA0002646